

Metal complexes of *N*-[Phenyl(pyrrolidin-1-yl)methyl]benzamide: Synthesis, Characterization and Antimicrobial Studies

L. MURUGANANDAM^{a*}, K. BALASUBRAMANIAN^a and K. KRISHNAKUMAR^b

^aDepartment of Chemistry, Saranathan College of Engineering, Tiruchirapalli-620 012, India

^bDepartment of Chemistry, National Institute of Technology, Tiruchirapalli-620 015, India
lmuruganandam@yahoo.co.in

Received 18 October 2012 / Accepted 12 November 2012

Abstract: A new series of vanadyl(IV), manganese(II), iron(II), nickel(II) and copper(II) complexes of *N*-[phenyl(pyrrolidin-1-yl)methyl]benzamide(PBB) have been synthesized and characterized by elemental analysis, molar conductance, IR, electronic, EPR spectra and magnetic measurements. Conductance measurements indicate that the above complexes are non-electrolytes. The spectral data show that, the ligand behaves as a neutral bidentate, bonded to metal ions via the carbonyl oxygen of acetamide group and azomethine nitrogen of morpholine moiety. Magnetic susceptibility measurements indicate tetrahedral geometry for Ni^{II} chloro, sulphato and Cu^{II} nitrate complexes and octahedral geometry for the rest. EPR spectral data suggest ionic link between metal center and the Mannich base ligand. IR studies indicate the presence of water molecules in some of the complexes. The antimicrobial studies show that the Cu^{II} complex is more active than others.

Keywords: Anticonvulsants, Axial perturbation, Multi-component, Pseudo tetrahedral

Introduction

There has been a growing interest in the chemistry of hydrazones and their metal complexes due to their application¹⁻⁶ as antifungal, antibacterial, anticonvulsant, antiinflammatory, antimalarial, analgesic, antipyretic, antituberculosis, anticancer activities and their use in treatment of leprosy⁷ and mental disorder diseases⁸. They act as herbicides, insecticides, nematocides, rodenticides and plant growth regulators, plasticizers and stabilizers for polymers, polymerization initiators and antioxidants⁹⁻¹¹. In analytical chemistry, they are being used in detection, determination and isolation of compounds containing carbonyl group¹². Much work on metal complexes of hydrazones with different functional groups has been reported¹³. However, little research has been done on metal complexes of the ligand under study, namely *N*-[phenyl(pyrrolidin-1-yl)methyl]benzamide (PBB). So, our work is devoted to the synthesis, characterization and antimicrobial studies of the ligand and its complexes with vanadyl(IV), manganese(II), iron(II), nickel(II) and copper(II).

Experimental

High purity Merck samples of acetamide, benzaldehyde and morpholine were used. All other solvents and metal salts were of A.R. grade and used as received.

Synthesis of the ligand

The new Mannich base ligand (PBB) was synthesized by employing the Mannich synthetic route¹⁴. Benzaldehyde (10 mL) followed by pyrrolidine (7.1 mL) was added to an ethanolic solution of benzamide (12.1 g) with constant stirring in an ice bath (1:1:1 mol ratio). After 20 days, the pale yellow solid obtained was washed with distilled water and then with acetone. The compound obtained was dried in an air oven and recrystallised from ethanol. The percentage yield was 86 (m.p. 76-80 °C). It was insoluble in water but completely soluble in all organic solvents.

Synthesis of the metal complexes

The hot methanolic solution of each of the metal salts was added slowly with constant stirring to the hot ethanolic solution of the ligand in 2:1 mol ratio. The insoluble complexes¹⁵ formed were filtered, washed with methanol and ethanol to remove the unreacted metal and ligand, dried in air and then in an air oven at 80 °C.

Instruments

C, H and N data were obtained with Carlo Erba 1108 elemental analyzer at RSIC, CDRI, Lucknow. Metal contents were estimated by the standard procedure and the results were further confirmed by atomic absorption spectroscopy. Sulphate was estimated gravimetrically and chloride was estimated volumetrically by Volhard's method¹⁶. The conductance data were obtained in $\sim 10^{-3}$ M DMF solutions of the complexes at room temperature using a Systronics direct reading digital conductivity meter-304 with dip type conductivity cell. IR spectra were recorded using a spectrum-one Perkin Elmer FT-IR spectrometer by using KBr pellets. The UV-Visible spectra were recorded in DMF solutions using double beam UV-Visible spectrometer, Perkin EZ-301 of working range 1100-190 nm. The ¹H and ¹³C NMR of the ligand were measured on a Bruker instrument and on a JEOL-GSX 400 spectrometer employing TMS as internal reference and DMSO-d₆ as solvent at ambient temperature. The FAB mass for the ligand was carried out using a JEOL GC mate mass spectrometer. X-band EPR spectra of Cu(II) complexes were recorded on a Varian E112 X-band spectrometer. The room temperature magnetic susceptibility measurements of the complexes were made by using a Guoy magnetic balance calibrated using mercury(II) tetrathiocyanatocobaltate(II).

Antibacterial and antifungal screening

Antibacterial activities¹⁷ of PBB and their sulphato metal complexes, namely VO^{IV}, Mn^{II}, Fe^{II}, Ni^{II} and Cu^{II} were tested *in vitro* against six bacterial species: *E. coli*, *P. aeruginosa* & *S. typhi* (Gram negative) and *B. subtilis*, *S. pyogenes* & *S. aureus* (Gram positive) and two fungal species: *A. niger* and *A. flavus* by disc diffusion method using agar nutrient as medium and gentamycin as control. The paper disc (3 mm) containing the compound (10, 20 and 30 µg/disc) was placed on the surface of the nutrient agar plate previously spread with 0.1 mL of sterilized culture of microorganism. After incubating this at 37 °C, for 24 h, the diameter of inhibition zone around the paper disc was measured. The zone of inhibition of the compounds is given in millimeter. The results obtained are tabulated in Tables 2&3.

Results and Discussion

Characterization of the ligand

The IR spectrum¹⁸ of PBB shows a strong band at 1634 cm^{-1} which may be attributed to the $\nu_{\text{C=O}}$ stretching mode. The other strong bands appearing at 1485, 1458 and 1210 cm^{-1} are assigned to bending vibrations of the (δ_{CH_2}) and stretching vibration of the pyrrolidine ring (ν_{ring}). The sharp peaks observed at 3346 cm^{-1} correspond to the ν_{NH} of the secondary amide group. The medium absorption band appearing at 1147 cm^{-1} in PBB pertain to the new C-N-C bond formed due to the formation of Mannich base by the insertion of pyrrolidinobenzyl group on benzamide. The absorption band present at 1186 & 1086 cm^{-1} in PBB may be assigned to the C-N-C frequency of pyrrolidine. It indicates the presence of monosubstitution of pyrrolidine in PBB.

UV-Vis spectrum¹⁹ of the compound in DMF registers an intense split bands centered at 263 and 235 nm which are presumably due to $n \rightarrow \pi^*$ transition of the carbonyl group and $\pi \rightarrow \pi^*$ transition of the carbonyl group and the benzene ring.

The ^1H NMR spectrum²⁰ shows ten signals of the protons of different groups at various regions. The chemical shift of the proton of $\text{N}(\text{CH}_2)_2$ at α , α^1 of pyrrolidine ring occurs at δ 2.56 ppm and that of the proton of $(\text{CH}_2)_2$ at β , β^1 of pyrrolidine occurs at δ 1.69 ppm. The signal at δ 8.92 ppm may be assigned to the secondary amide NH proton. The methine proton shows a doublet at δ 5.86 and δ 5.83 ppm. The multiplet in the range δ 7.93-7.25 ppm is attributed to the protons of the benzene ring. The signals at δ 7.93, 7.88 and 7.54 ppm may be assigned to the CH of benzamide at positions 2 & 6, 4 and 3 & 5 respectively and the chemical shift of the protons of aldehydic benzene ring occurs at δ 7.48, 7.36 and 7.25 ppm of positions 2 & 6, 3 & 5 and 4 respectively. Thus this spectrum reveals the presence of phenyl, pyrrolidino, amido NH and methine groups in the compound.

According to the ^{13}C NMR spectrum²¹ obtained, the carbonyl carbon shows a signal at δ 168.39 ppm. The signals observed between δ 134.83 - 127.95 ppm are due to aromatic carbons of benzamide. The resonance signals at δ 134.83, 131.70, 128.66 and 127.91 ppm are assigned to the carbons of the phenyl group at 1, 4, 3 & 5 and 2 & 6 positions. The substituted carbon of the aromatic ring can be distinguished by its decreased peak height (δ 134.83 ppm). The aromatic carbons of aldehydic moiety at 1, 2 & 6, 3 & 5 and 4 gives signals at δ 141.58, 128.07, 128.58 and 127.75 ppm respectively. The signals due to the C_1 carbon of benzene ring can be differentiated by its decreased peak height (δ 141.58 ppm). The molecular mass of the compound determined by the Rast method 278.97 is close to the expected value of 280.

The mass spectrum²² of PBB obtained on Electron Ionization mode, shows a very weak molecular ion peak at $m/z = 280$, which confirms the assigned molecular mass to this Mannich base. Thereupon on fragmentation it records intense signals at $m/z = 204$ & $m/z = 126$ which are due to the removal of C_6H_5^- and C_6H_5^- groups respectively. The next m/z signal at 82 is due to the removal of HCONH^- ion. Finally the signal at $m/z = 69$ is due to the presence of pyrrolidine ion. Based on the data obtained from various physical and chemical studies, the molecular structure of PBB is shown in Figure 1.

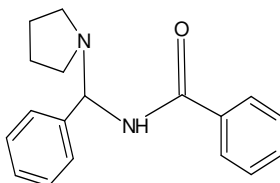


Figure 1. *N*-[Phenyl(pyrrolidin-1-yl)methyl]benzamide

Characterization of the complexes

To find out the stoichiometry²³ of the complexes, the percentage of the metal ions, anions and CHN were determined. The electrical conductance measurements of the complexes were done in order to ascertain whether the anion is within or outside the coordination sphere of the complex. The molar conductance values are seen that, all the complexes are non-electrolytes. The CHN analyses are also in good agreement with the calculated values. The percentages of the CHN, metal ions & anions and molar conductance data of the complexes are presented in Table 1.

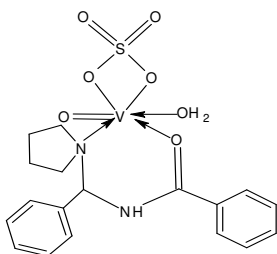
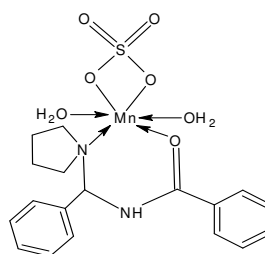
Table 1. Analytical and Conductance Data for V^{IV}, Mn^{II}, Fe^{II}, Ni^{II} and Cu^{II} Complexes of PBB

Complex	% C		% H		% N		%Metal		%Anion		Λ_M ohm ⁻¹ cm ² mol ⁻¹
	Obs.	(Cal.)	Obs.	(Cal.)	Obs.	(Cal.)	Obs.	(Cal.)	Obs.	(Cal.)	
VOSO ₄ .PBB.	38.70		4.12		4.85		8.99		18.10		31.65
H ₂ O	(39.20)		(3.63)		(5.08)		(9.25)		(17.42)		
MnSO ₄ .	39.32		4.04		4.75		10.63		18.00		19.82
PBB.2H ₂ O	(40.07)		(3.71)		(5.19)		(10.19)		(17.42)		
FeSO ₄ .PBB.	36.68		3.10		5.08		9.16		16.97		24.07
2H ₂ O	(36.36)		(3.37)		(4.71)		(9.40)		(16.16)		
NiCl ₂ .PBB	42.34		3.29		5.01		10.89		14.19		43.13
	(41.70)		(3.86)		(5.41)		(11.33)		(13.68)		
Ni(NO ₃) ₂ .	38.00		3.90		5.12		9.95		22.14		15.49
PBB	(37.83)		(3.50)		(4.91)		(10.28)		(21.72)		
Cu(NO ₃) ₂ .	39.32		4.19		4.96		12.07		21.85		29.41
PBB.2H ₂ O	(38.71)		(3.94)		(5.02)		(11.39)		(22.22)		
CuSO ₄ .PBB	41.22		4.09		4.95		11.74		18.81		12.55
	(40.83)		(3.78)		(5.29)		(12.01)		(18.15)		

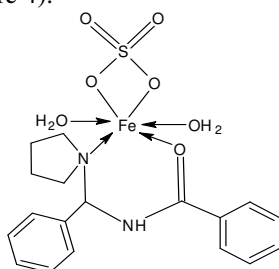
The IR spectra of the complexes registered lower frequency values for the C=O and CNC by about 126 - 06 cm⁻¹ (when compared to the free ligand values), which suggests the bidentate coordination of the ligand. The vanadyl complex display a strong V=O stretching²⁴ at 771 cm⁻¹. The ν_3 of sulphato group appears a broad band at 1154 - 996 cm⁻¹. The ν_4 appears at 682 - 603 cm⁻¹. The ν_1 and ν_2 mode of coordinated sulphato group occurs at 865 - 771 and 536-475 cm⁻¹ respectively. These bands observed in all the complexes were associated with the bidentate chelating sulphato group. The complexes show bands at 3657-3656, 1645-1622, 835-771, 682-653 and 536-457 cm⁻¹ respectively, which are assigned as ν_{OH} , δ_{HOH} , ρ_{rHOH} , ρ_{wHOH} and ν_{M-O} modes respectively, of coordinated water²⁵ in sulphato complexes of vanadium, manganese and iron and nitrate complex of copper

The UV-Visible spectrum of vanadyl complex shows the absorption bands at 14499, 16602 and 27030 cm⁻¹ which indicate the presence of the axial V=O bond²⁶. This axial perturbation leads to the splitting of the energy levels into three possible transitions are ${}^2B_2 \rightarrow {}^2E_2$, ${}^2B_2 \rightarrow {}^2B_1$ and ${}^2B_2 \rightarrow {}^2A_1$. The EPR spectrum²⁷ of this complex shows only one resolution at g_{\parallel} region; so it can be assumed that g_x and g_y are same or nearly the same. The g value of 1.8903 for oxovanadium(IV) indicate a strong interaction between the ligand and the metal ion. The room temperature magnetic moment value is 1.57 B.M. which suggests a hexa coordinate geometry around VO^{IV} ion (Figure 2).

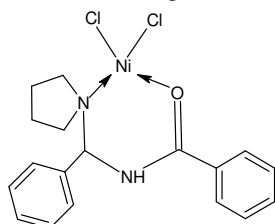
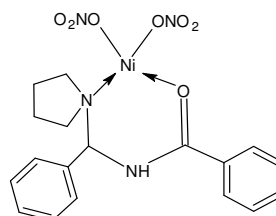
The UV-Visible spectrum of manganese complex shows four absorption bands at 18049 cm⁻¹ due to ${}^6A_{1g} \rightarrow {}^4T_{1g}(G)$ transition, at 24986 cm⁻¹ due to ${}^6A_{1g} \rightarrow {}^4E_g$, ${}^4A_{1g}(G)$ transition, at 29135 cm⁻¹ due to ${}^6A_{1g} \rightarrow {}^4E_g(D)$ transition and at 31274 cm⁻¹ due to ${}^6A_{1g} \rightarrow {}^4T_{1g}(P)$ transitions respectively. The room temperature magnetic moment value is found to be 5.96 B.M. These observations suggest a high spin octahedral geometry²⁸ for the complex (Figure 3).

**Figure 2.** VOSO₄.PBB.H₂O**Figure 3.** MnSO₄.PBB.2H₂O

The UV-Visible spectrum of iron exhibits a strong intense band at 11258 cm⁻¹ which is due to ⁵T_{2g}→⁵E_g transition and a CT band at 23402 cm⁻¹ which obscures the other very low intensity d-d absorption bands. The μ_{eff.} value of 5.67 B.M. conforms to a hexa coordinate geometry²⁸ around Fe^{II} ion (Figure 4).

**Figure 4.** FeSO₄.PBB.2H₂O

The nickel chloro and nitrate complexes exhibits band at 3917 & 3870 cm⁻¹ due to ³T_{1g}(F)→³T_{2g}(F) transition, at 8402 & 8413 cm⁻¹ due to ³T_{1g}(F)→³A_{2g}(F) transition and at 15036 & 15389 cm⁻¹ due to ³T_{1g}(F)→³T_{2g}(P) transition respectively. The charge transfer transition band occurs at 25675, 28561 & 24555 cm⁻¹. The ν₂/ν₁ ratio for the chloro and nitrate complexes are 2.17 and 2.15. The μ_{eff.} values for the chloro and nitrate complexes of Ni^{II} are 3.80 and 4.36 B.M. indicating tetrahedral environment (Figure 5&6) around Ni^{II} ion²⁹.

**Figure 5.** NiCl₂.PBB**Figure 6.** Ni(NO₃)₂.PBB

The sulphato complex of Cu^{II} exhibit electronic absorption band at 9145 cm⁻¹ due to ²B_{1g}→²A_{1g} transition at 11078 cm⁻¹ due to ²B_{1g}→²B_{2g}, at 12804 cm⁻¹ due to ²E_g→²T_{2g}(F) and the bands observed at 34472 & 35699 cm⁻¹ may be due to charge transfer transitions. The band positions and multi-component nature of the spectra suggest a tetrahedral geometry³⁰. Nitrate complex of Cu^{II} exhibit electronic absorption bands at 8245 cm⁻¹ due to ²B_{1g}→²A_{1g}, 11328 cm⁻¹ due to ²B_{1g}→²B_{2g}, 14650 cm⁻¹ due to ²E_g→²T_{2g}(F) and the bands at 26392 & 35675 cm⁻¹ are assigned due to charge transfer transitions (ligand→metal) respectively. The band positions and multi-component nature of the spectra suggest a tetragonally distorted octahedral geometry³¹ to the above complex.

The μ_{eff} value of sulphato complex is 2.78 B.M. suggests the distorted tetrahedral geometry. The μ_{eff} value (1.89 B.M.) of nitrate complex indicate that the complex is magnetically diluted and have distorted octahedral geometry.

The X band EPR spectra of polycrystalline chloro, nitrate and sulphato complexes of Cu^{II} are recorded at LNT (77 K). The g_{\parallel} values of nitrate and sulphato complexes are less than 2.30 indicating the covalent nature. The higher g_{\parallel} values may be due to the coordination of H_2O to the Cu^{II} ion in these complexes. The axial symmetry parameter G value which is a measure of interaction between the metal centers in the crystalline solids for the sulphato complex of Cu^{II} is 4.95 and this suggests the lack of change interaction between two Cu^{II} centres in the unit cell of the complex³². The value of G is less than 4 for nitrate complex of Cu^{II} and it show considerable coupling and appreciable misalignment of the local tetragonal axes leading to an exchange interaction of free electron between two copper centers in the solid state. Based on the above discussions six coordinated tetragonally distorted octahedral geometry (Figure 7) may be assigned to nitrate complex and pseudo tetrahedral structure³³ for sulphato complex (Figure 8) of Cu^{II} .

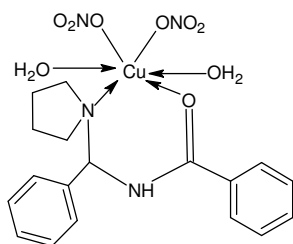


Figure 7. $\text{Cu}(\text{NO}_3)_2 \cdot \text{PBB} \cdot 2\text{H}_2\text{O}$

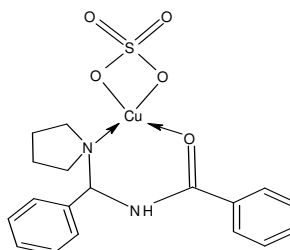


Figure 8. $\text{CuSO}_4 \cdot \text{PBB}$

A comparison of diameters of the inhibition zones of the compounds investigated and listed in Table (2) and (3). Cu^{II} sulphato complex shows highest antibacterial and antifungal activity against all the species studied. They have larger diameters of inhibition zones than the control at the same concentration and identical conditions. This observation indicates that chelation increases the activity of the complex. The higher activity of the Cu^{II} complex may be due to the fact that, during transcription and transformation of nuclei acids, copper is an essential micronutrient. Cu^{II} complex was shown to inhibit cellular protein and RNA synthesis. In Cu^{II} complex the labile water can exchange its coordination sites with the enzymatic $-\text{SH}$ group and hence inhibits the bacterial growth³⁴.

Table 2. Antibacterial activity of ligand and its complexes

Compound	<i>Escherichia coli</i>			<i>Pseudomonas aeruginosa</i>			<i>Salmonella typhi</i>			<i>Bacillus subtilis</i>			<i>Streptococcus pyogenes</i>			<i>Staphylococcus aureus</i>		
	10	20	30	10	20	30	10	20	30	10	20	30	10	20	30	10	20	30
Conc. ($\mu\text{g}/\text{disc}$)	10	20	30	10	20	30	10	20	30	10	20	30	10	20	30	10	20	30
Control	10	14	17	10	13	17	12	14	19	11	14	16	10	12	16	11	13	17
PBB	12	16	19	11	14	19	15	16	20	11	15	18	12	14	18	13	16	19
$\text{VO}_4 \cdot \text{PBB} \cdot \text{H}_2\text{O}$	15	18	20	12	15	21	15	18	23	13	16	20	13	16	20	14	18	22
$\text{MnSO}_4 \cdot \text{PBB} \cdot 2\text{H}_2\text{O}$	16	18	21	14	16	23	17	20	25	15	19	23	15	19	25	16	21	28
$\text{FeSO}_4 \cdot \text{PBB} \cdot 2\text{H}_2\text{O}$	18	20	23	17	19	26	18	21	28	18	21	25	17	22	29	19	27	32
$\text{CuSO}_4 \cdot \text{PBB}$	21	26	30	19	23	29	23	28	34	23	29	35	21	27	38	25	31	36

Table 3. Antifungal activity of ligand and its complexes

Compound	<i>A. niger</i>			<i>A. flavus</i>		
	10	20	30	10	20	30
Conc. ($\mu\text{g}/\text{disc}$)	10	20	30	10	20	30
Control	8	9	12	5	9	12
PBB	9	12	16	8	11	17
VOSO ₄ .PBB.H ₂ O	11	15	21	13	16	24
MnSO ₄ .PBB.2H ₂ O	15	19	26	16	19	28
FeSO ₄ .PBB.2H ₂ O	18	22	28	17	23	34
CuSO ₄ .PBB	21	27	35	23	29	37

The fungi toxicity of the free ligand is less severe than that of the metal chelates. A possible mechanism of toxicity may be speculated in the light of chelation theory. Chelation reduces considerably the polarity of the metal ion mainly because of partial sharing of its positive charge with donor groups and possible π -delocalization of electron over the chelate ring. This increases the lipophilic character of the neutral chelate which favours its permeation through lipid layers of fungus membranes. Furthermore, the mechanism of action of the compounds may involve the formation of hydrogen bond through the uncoordinated hetero atoms O, S and N with the active centers of the cell constituents resulting in the interference with the normal cell process³⁵. Presence of lipophilic and polar substituents like C=O, NH, *etc.*, are expected to enhance the fungi toxicity.

Conclusion

The ligand, *N*-[Phenyl(pyrrolidin-1-yl)methyl]benzamide and its complexes of vanadyl(IV), manganese(II), iron(II), nickel(II) and copper(II) were synthesized and characterized. Based on the spectral data, the ligand behaves as bidentate through the CO of acetamide group and CNC of morpholine moiety. The UV-Vis and magnetic susceptibility measurements indicate the tetrahedral geometry for Ni^{II} chloro, sulphato and Cu^{II} nitrate complexes and octahedral geometry for the rest of the metal complexes. IR studies indicate the presence of water molecules in some of the complexes. The antimicrobial screening shows that the Cu^{II} complex is more active than others due to vital role in transcription and transformation of cell process.

Acknowledgement

The authors express their sincere thanks to the Secretary, Principal and Dean(R&D), Saranathan College of Engineering, Tiruchirapalli for providing facilities and motivating them. A part of the work was carried out at NIT, Tiruchirapalli.

References

1. Macias B, Villa M V, Gomez B, Joaquín Borrás, Alzuet G, Marta González-Álvarez and Alfonso Castiñeiras, *J Inorg Bio Chem.*, 2007, **101(3)**, 444-451.
2. Haidne L and Cristian Silvestru, *Coord Chem Rev.*, 1990, **99**, 253-296.
3. Filion G J P, Zhenilo S, Salozhin S, Yamada D, Prokhortchouk E and Defossez P A, *Mol Cell Biol.*, 2006, **26**, 169-181.
4. Liu C, Wang M, Zhang T and Sun H, *Coord Chem Rev.*, 2004, **248(1-2)**, 147-168.
5. Dizdaroglu M, *Free Radical Biol Med.*, 1991, **10(3-4)**, 225-242.
6. Belaid S, Landreau A, Djebbar S, Ouassini Benali-Baitich, Gilles Bouet and Jean-Philippe Bouchara, *J Inorg Bio Chem.*, 2008, **102(1)**, 63-69.
7. Sigel H, *Metal Ions in Biological Systems*; Marcel Dekker Inc.; New York, 1980.
8. Humphreys K J, Johnson A E, Karlin K D and Rokita S E, *J Biol Inorg Chem.*, 2002, **7(7-8)**, 835-842.

9. Garca Raso A, Fiol J J, Adrover B, Virtudes Moreno, Ignasi Mata, Enrique Espinosa and Elies Molins, *J Inorg Biochem.*, 2003, **95(2-3)**, 77-86.
10. Wang X-L, Chao H, Li H, Xian-Lan Hong, Liang-Nian Ji and Xiao-Yuan Li, *J Inorg Biochem.*, 2004, **98(3)**, 423-429.
11. Brown D H, Lewis A J, Smith A E and Teape J W, *J Med Chem.*, 1980, **23(7)**, 729-734.
12. Liu J, Zhang H and Chen C, *Dalton Trans.*, 2003, **114**, 26.
13. Pandit L, *J Indian Council Chem.*, 1995, **11**, 57.
14. Tramontini M and Angiolini L, *Tetrahedron*, 1990, **46(6)**, 1791-1837.
15. Billing D E, Hathaway B J and Bew M J, *J Chem Soc A*, 1970, 18, 77.1090-1095; DOI: 10.1039/J19700001090
16. Vogel A I, Quantitative Chemical Analysis, 6th Edn., 2004, 465.
17. Hirohama T, Kuranuki Y, Ebina E, Takashi Sugizaki, Hidekazu Aarii, Makoto Chikira, Pitchumony Tamil Selvi and Mallayan Palaniandavar, *J Inorg Biochem.*, 2005, **99(5)**, 1205-1219.
18. Nakamoto K, "*Infrared and Raman Spectra of Inorganic and Coordination Compounds*", 5th Edn., John Wiley & Sons, Toronto, 1997 Part B, 60.
19. Parkin G, *Chem Rev.*, 2004, **104(2)**, 699-768.
20. Wang M Z, Meng Z X, Liu B L, Guan-Liang Cai, Chun-Li Zhang and Xiang-Yun Wang, *Inorg Chem Commun.*, 2005, **8(4)**, 368-371.
21. Sharma V K, Pandey O P and Sengupta S K, *Trans Met Chem.*, 1987, **12**, 509.
22. Yongsheng Hu, Zhaoxiang Wang, Hong Li, Xuejie Huang and Liquan Chen, *Int J Mass Spectr.*, 2006, **255**, 251-264.
23. Viswanathamurthi P, Dharmaraj N and Natarajan K, *Synth React Inorg Met Org Chem.*, 2000, **30(7)**, 1273-1285.
24. Frey S T, Sun H H H, Murthy N N and Karlin D K, *Inorg Chim Acta*, 1996, **242(1-2)**, 329-338.
25. Savinkina E, Albov D, Buravlev E and Zamilatskov I, *Russian J Inorganic Chem.*, 2007, **52**, 1056-1062.
26. Humphreys K J, Karlin K D and Rokita S E, *J Am Chem Soc.*, 2002, **124(21)**, 6009-6019.
27. Wertz J E and Bolton J R, "*ESR Elementary Theory and Practical Applications*", Chapman and Hall, New York, 1986.
28. Seigel H and Martin R B, *Chem Rev.*, 1982, **82(4)**, 385-426.
29. Raman N, Sakthivel A and Rajasekaran K, *J Coord Chem.*, 2009, **62**, 1661.
30. Penner-Hahn J E, *Indian J Chem A*, 2002, **41**, 13-21.
31. Cozzi P G, *Chem Soc Rev.*, 2004, **33**, 410-421.
32. Kasuga N C, Yamamoto R, Hara A, Amano A and Nomiya K, *Inorg Chim Acta*, 2006, **359(13)**, 4412-4416.
33. Chabner B A, *J Natl Cancer Inst.*, 1990, **82(13)**, 1083-1085.
34. Singh K, Barwa M S and Tyagi P, *Eur J Med Chem.*, 2007, **42(3)**, 394-402.
35. Chohan Z H, Hassan M U I, Khan K M and Supuran C T, *J Enzyme Med Chem.*, 2005, **20**, 183.